Absorption mechanisms in the gamma-ray binary LS 5039 from its full radio spectrum

Marcote et al. (2015), MNRAS, in press (arXiv:1504.07253)

Benito Marcote

M. Ribó, J. M. Paredes, C. H. Ishwara-Chandra

Variable Galactic Gamma-ray Sources
May 4, 2015

Universitat de Barcelona

ICCUB
Institut de Ciències del Cosmos

Gamma-Ray Binaries

Binary systems which host a compact object orbiting a high mass star that have the non-thermal maximum of the Spectral Energy Distribution in γ-rays. (Paredes et al. 2013, Dubus 2013)

System	Main star	P/ days
LS 5039	06.5 V	3.9
1FGL J1018.6–5856	O6 V	16.6
LS I +61 303	B0 Ve	26.5
HESS J0632+057	B0 Vpe	315.0
PSR B1259–63	09.5 Ve	1236.7
Cygnus X-3	WR	0.2
Cygnus X-1 ??	09.7 Ve	5.6
MWC 656 ??	Be	60.4

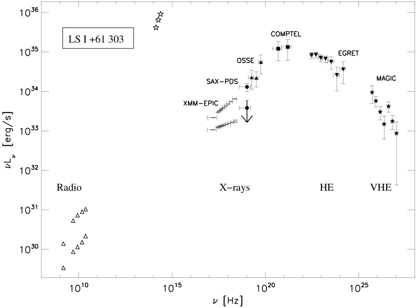

Red: known gamma-ray binaries
Green: X-ray binaries with gamma-ray emission

Gamma-Ray Binaries

Binary systems which host a compact object orbiting a high mass star that have the non-thermal maximum of the Spectral Energy Distribution in γ-rays. (Paredes et al. 2013, Dubus 2013)

System	Main star	P/ days
LS 5039	06.5 V	3.9
1FGL J1018.6–5856	O6 V	16.6
LS I +61 303	B0 Ve	26.5
HESS J0632+057	B0 Vpe	315.0
PSR B1259–63	09.5 Ve	1236.7
Cygnus X-3	WR	0.2
Cygnus X-1 ??	09.7 Ve	5.6
MWC 656 ??	Be	60.4

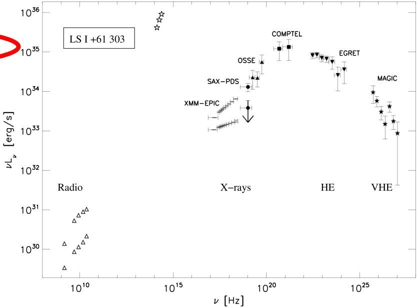

Red: known gamma-ray binaries

Green: X-ray binaries with gamma-ray emission

Understanding the emission of Gamma-Ray Binaries

Young non-accreting pulsar scenario

Strong shock between both winds:

- Relativistic pair plasma wind from the pulsar
- Stellar wind from the massive companion star

Originally proposed by Maraschi & Treves (1981), re-proposed by Dubus (2006)

- **High energy** emission produced by synchrotron and inverse Compton.
- **Radio flux** dominated by the synchrotron emission

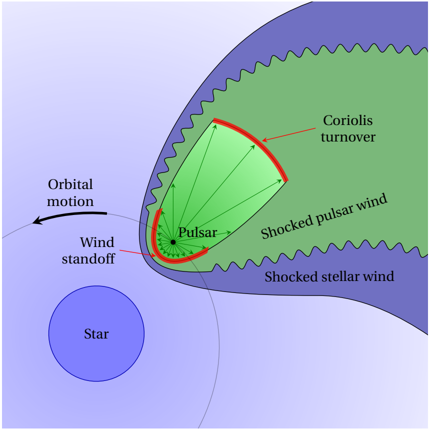

Model for LS 5039 (Zabalza et al. 2012)

The gamma-ray binary LS 5039

$\alpha_{\rm J2000} = \ \ 18^{\rm h}\ 26^{\rm m}\ 15.06^{\rm s}$
$\delta_{\rm J2000} = -14^\circ\ 50'\ 54.3''$

O6.5 V main-sequence star ($23 \pm 3\ \rm M_\odot$)
Compact object, NS or BH (1–$5\ \rm M_\odot$)

$P \approx 3.9$ d
$e = 0.35 \pm 0.04$
$d = 2.5 \pm 0.5$ kpc

TeV light-curve: periodic
GeV light-curve: periodic (anticorrelated)
X-rays: periodic
Radio: persistent, small variability without orbital modulation

Clark et al. (2001), Aharonian et al. (2005), Casares et al. (2005), Kishishita et al. (2009), Abdo et al. (2009), Casares et al. (2012), Zabalza et al. (2013)

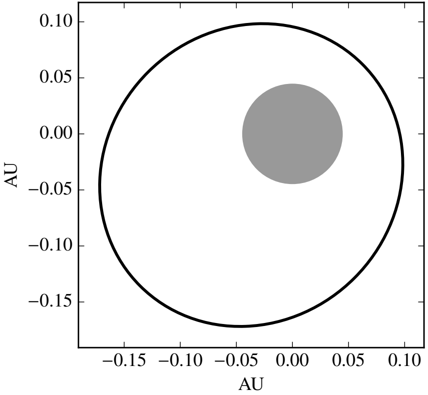

Previous radio observations of LS 5039

- Variability from Martí et al. (1998)

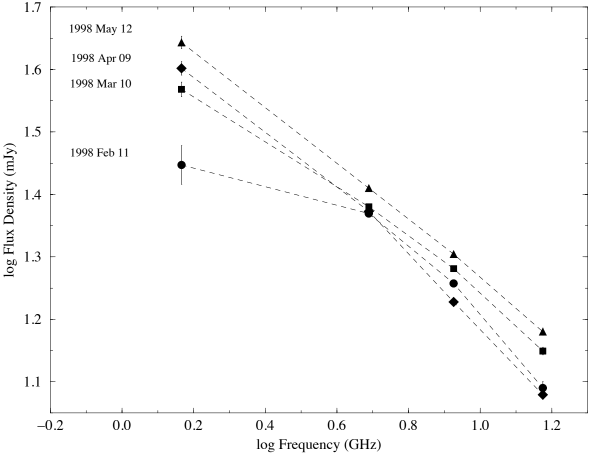

Spectral index $\alpha = -0.46 \pm 0.01$, variability $< \pm 25$ %

Previous radio observations of LS 5039

- VLBI observations: Moldón et al. (2012)

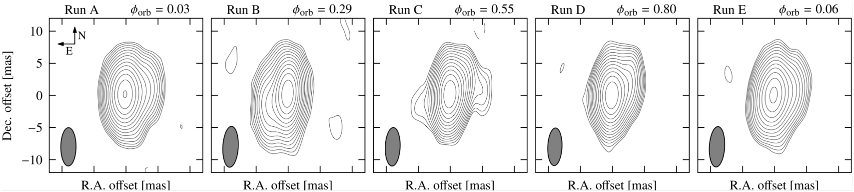

Observations along one orbital period

Dominant core emission ($\lesssim$ 1 mas, or 3 AU) + extended emission orbitally modulated

Previous radio observations of LS 5039

- At low frequencies, only a few observations have been published with contradictory results.

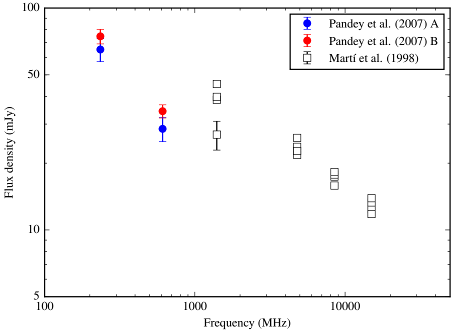

Adapted from Pandey et al. (2007)

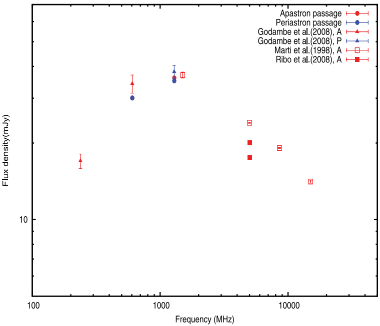

Bhattacharyya et al. (2012)

Godambe et al. (2008)

Radio observations

Work published in Marcote et al. (2015)

- 1.4 – 15 GHz (VLA)
  Monitoring in 2002

- 154, 235 & 610 MHz (GMRT)
  Archival observations 2004–08

- 154 MHz – 5 GHz (GMRT & WSRT)
  Two quasi-simultaneous observations in 2013.

Accurate GMRT data reduction

Analyzing the GMRT data we found the reasons of the differences between Pandey et al. (2007) and Godambe et al. (2008):

- At low frequencies, the contribution of the Galactic diffuse emission is quite high within the Galactic Plane.
- It must be removed to recover the right flux densities in the final image. Otherwise the flux densities will be underestimate.
- Usually done automatically in most telescopes. Not in the GMRT.
- Godambe et al. (2008) did not take into account this correction.
- Pandey et al. (2007) used the Haslam approximation (see Marcote et al. 2015), extrapolating the emission seen at 408 MHz.
- We have conducted dedicated non correlated observations with the GMRT to directly measure the Galactic contribution in the field of LS 5039 to properly substract it.
- We have seen significant differences in these two methods for the field of LS 5039 (compatible with the comparison in Sirothia 2009).

Accurate GMRT data reduction

Analyzing the GMRT data we found the reasons of the differences between Pandey et al. (2007) and Godambe et al. (2008):

- At low frequencies, the contribution of the Galactic diffuse emission is quite high within the Galactic Plane.
- It must be removed to recover the right flux densities in the final image. Otherwise the flux densities will be underestimate.
- Usually done automatically in most telescopes. Not in the GMRT.
- Godambe et al. (2008) did not take into account this correction.
- Pandey et al. (2007) used the Haslam approximation (see Marcote et al. 2015), extrapolating the emission seen at 408 MHz.
- We have conducted dedicated non correlated observations with the GMRT to directly measure the Galactic contribution in the field of LS 5039 to properly substract it.
- We have seen significant differences in these two methods for the field of LS 5039 (compatible with the comparison in Sirothia 2009).

CALIBRATION RELATED PROBLEMS!

Summary of the observations analyzed in this work

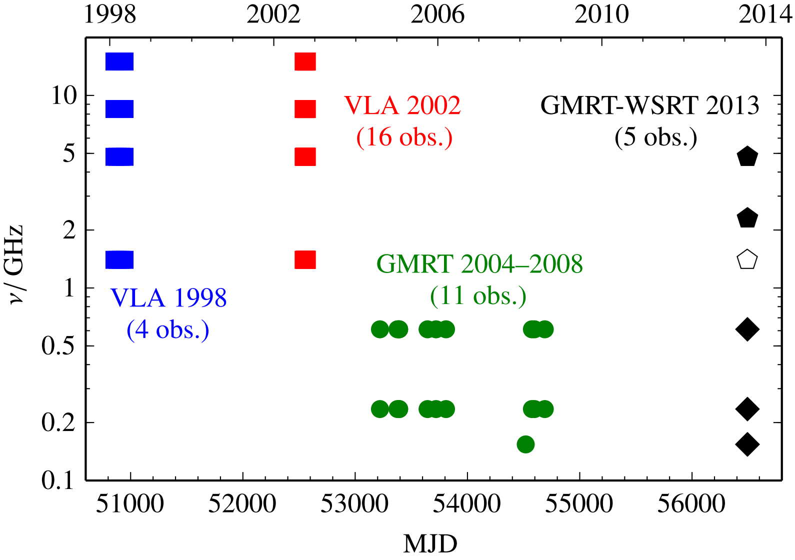

Summary of the observations analyzed in this work

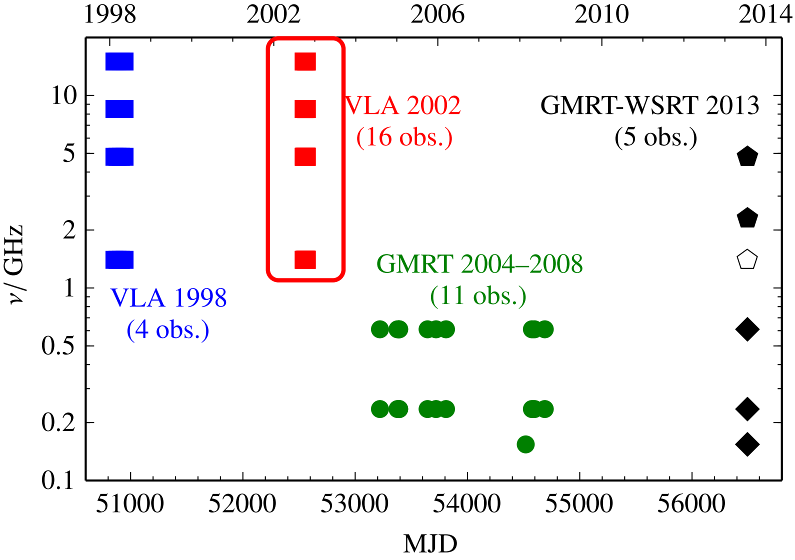

High-frequency variability along the orbit

VLA monitoring in 2002

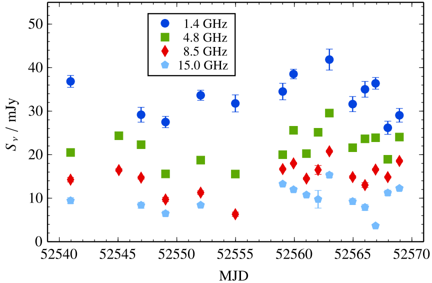

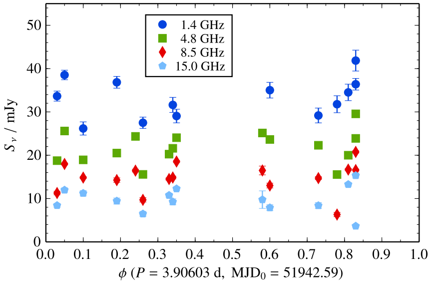

- Persistent flux density emission.
- Variability on timescales as short as one day.

- No visible orbital modulation
- Variability $< \pm 25$ %

Flux density values at all frequencies compatible with the ones reported at other epochs (e.g. Martí et al. 1998).

High-frequency variability along the orbit

VLA monitoring in 2002

- Dashed lines represent the power-laws determined from 5.0 and 8.5 GHz
- We observe a ≈ power-law at these GHz frequencies most of the times
- Slight curvature below 2 GHz
- Average spectral index: $\alpha = -0.57 \pm 0.12$

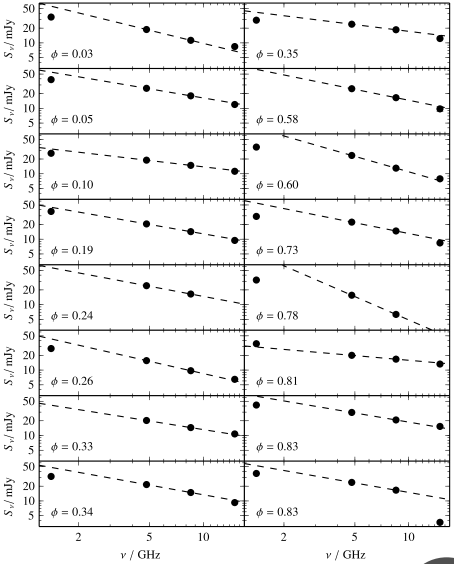

Low-frequency variability along the orbit

Archival GMRT observations 2004–2008

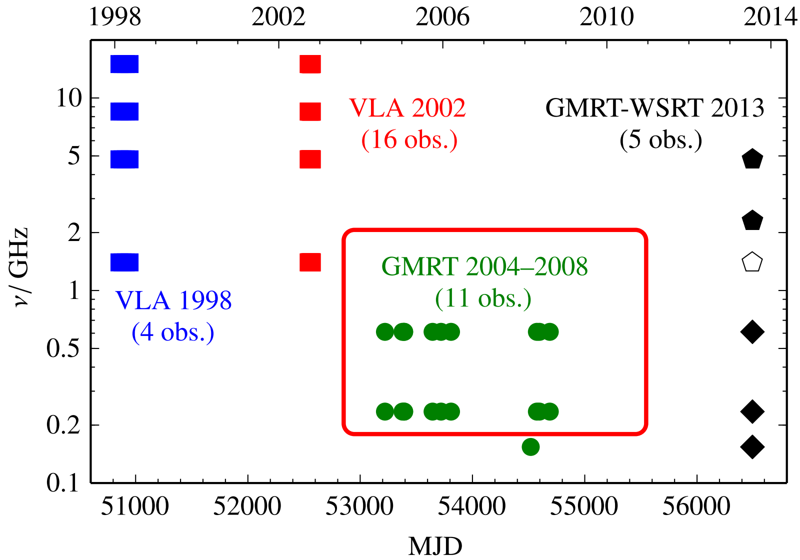

Low-frequency variability along the orbit

Archival GMRT observations 2004–2008

- Observations spread over 4 yr
- Persistent emission
- Variability at $> 6\sigma$
- Average spectral index
  $\alpha = +0.5 \pm 0.8$
- Hints of orbital modulation?

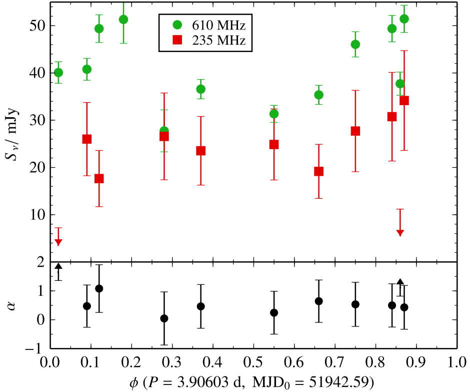

Non-simultaneous spectrum of LS 5039

Combining data from 1998 to 2013

- Small variability along the years ($< 25\,\% \quad \forall\ \nu$)
- "Similar" profile in average
- Turnover at ~ 0.5 GHz
- Source undetected at 150 MHz

- Only two data at 2.3 GHz (no statistics)
- The mean square errors have been used in the average data

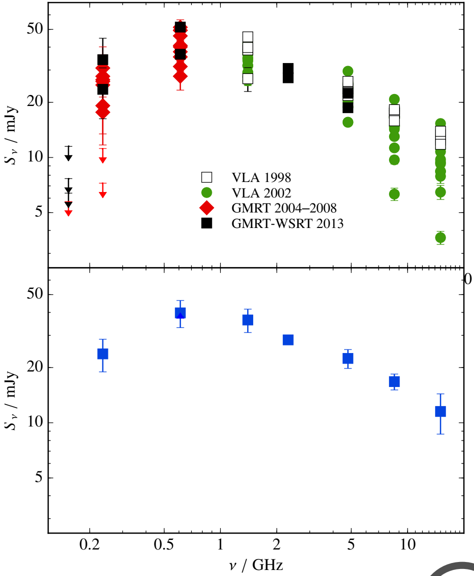

Modeling the LS 5039 spectrum

A first approximation (toy model)

From VLBI observations (Moldón et al. 2012) we known that most of the radio emission comes from a compact core $\lesssim 1$ mas (~ 3 AU).

We have built a very simple model to understand the spectrum:

- Compact core $\rightsquigarrow$ one-zone model
- No orbital modulation $\rightsquigarrow$ symmetric emitting region (spheric)
- For simplicity $\rightsquigarrow$ isotropic and homogeneous
- We consider the presence of a synchrotron emitting plasma
- Turnover produced either by SSA, FFA or Razin effect (and combinations of them)

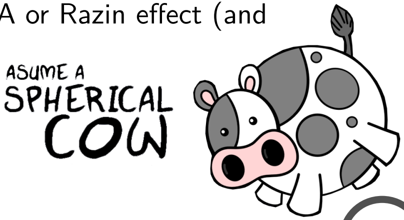

Modeling the LS 5039 spectrum

A first approximation (toy model)

We have built a very simple model to understand the spectrum:

- Synchrotron emission, with a particle injection:

$$n(E)\mathrm{d}E = KE^{-p}\mathrm{d}E$$

- Synchrotron self-absorption (SSA):

$$\kappa_{\mathrm{SSA}} \propto KB^{(p+2)/2}\nu^{-(p+4)/2}$$

- Free-free absorption (FFA):

$$\kappa_{\mathrm{FFA}} \propto n_{\mathrm{e}}^2 T_{\mathrm{w}}^{-3/2}\nu^{-2}$$

- Razin effect:

$$S_\nu \rightsquigarrow S_\nu e^{-\nu_{\mathrm{R}}/\nu}, \qquad \nu_{\mathrm{R}} \equiv 20 n_{\mathrm{e}} B^{-1}$$

Non-simultaneous spectrum of LS 5039

Combining data from 1998 to 2013

- The average spectrum can be fitted by typical models:
  - SSA
  - Synchrotron + FFA
  - SSA + Razin
  - FFA + Razin
  - SSA + FFA
- SSA+Razin effect is the best fit to the data
- Small differences between all of them

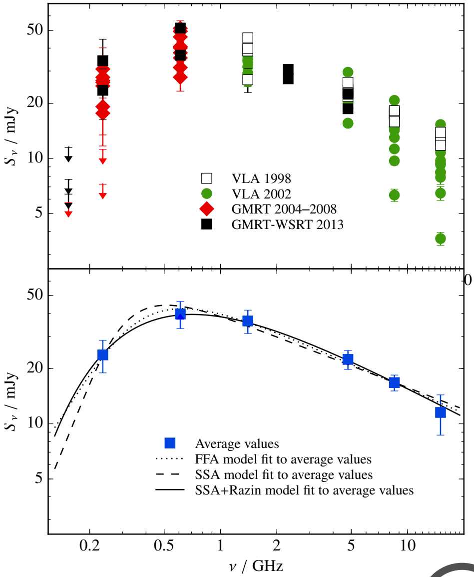

Quasi-simultaneous spectrum of LS 5039

GMRT & WSRT campaign in 2013 July 19 and 21

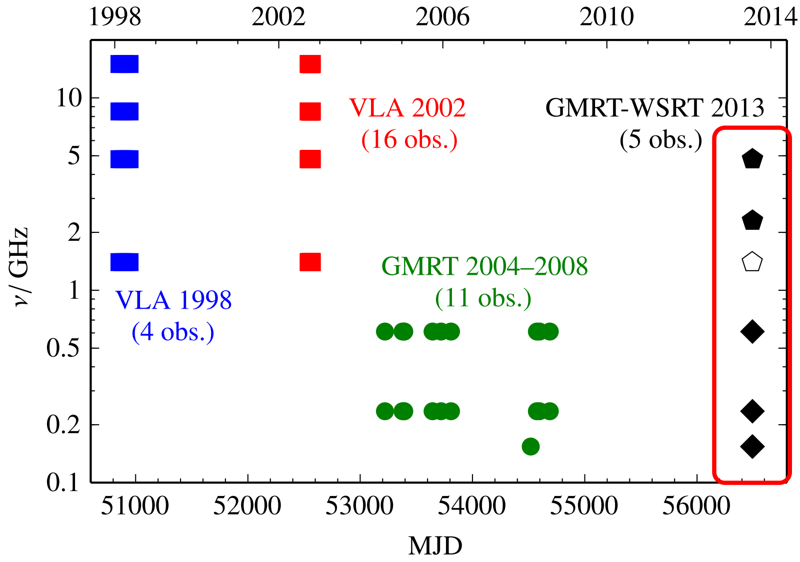

Quasi-simultaneous spectrum of LS 5039

GMRT & WSRT campaign in 2013 July 19 and 21

Two 0.15–5 GHz spectra at orbital phases $\phi \approx 0.9$ and 0.4.

- Although similar to the average spectrum, we observe subtle differences between the two epochs.
- The turnover at ~ 0.5 GHz is persistent.
- Stronger emission on 2013 July 19.
- 2013 July 19: pure SSA spec.
- 2013 July 21: SSA+Razin spec.
- FFA provides poor fits

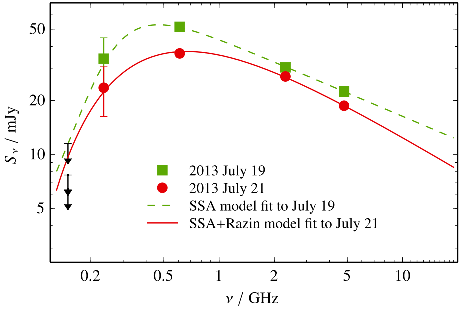

GMRT data: 235 and 610 MHz
WSRT data: 2.3 and 5.0 GHz

154 MHz GMRT data taken every other day (on 2013 July 18, 20 and 22)

Modeling the LS 5039 spectrum

The three spectra show a similar shape but with subtle differences:

- Avg. spectrum: SSA+Razin
- July 19 spectrum: SSA
- July 21 spectrum: SSA+Razin

Fit	p	$\Omega B^{-1/2}$ $\left[10^{-16}\,\mathrm{G}^{-1/2}\right]$	$K\ell B^{(p+2)/2}$ $\left[10^{3}\,\mathrm{cm}\,\mathrm{G}^{(p+2)/2}\right]$	ν_{R} $[10^{8}\,\mathrm{Hz}]$
Avg. spectrum	2.16 ± 0.04	500 ± 800	3 ± 5	4.1 ± 0.2
July 19	1.867 ± 0.014	3.9 ± 0.3	$(2.1 \pm 0.9) \times 10^{6}$	–
July 21	2.24 ± 0.08	200 ± 600	0.4 ± 1.7	4.1 ± 0.7

- We can also compare these results with the free-free opacity inferred from the stellar wind (the region must be optically thin to FFA)

Modeling the LS 5039 spectrum

Building a coherent picture from the fits and the free-free opacity:

- Avg. spectrum: SSA+Razin
- July 19 spectrum: SSA
- July 21 spectrum: SSA+Razin
- Coherent picture with:

$$\ell \sim 0.85 \text{ mas} (\sim 2.5 \text{ AU})$$
$$B \sim 20 \text{ mG}$$
$$n_e \sim 4 \times 10^5 \text{ cm}^{-3}$$
$$\dot{M} \sim 5 \times 10^{-8} \text{ M}_\odot \text{ yr}^{-1}$$

where:

ℓ: linear size of the emitting region,
B: module of the magnetic field,
n_e: electron density of the non-relativistic plasma,
$\dot{M}$: mass-loss rate of the companion star.

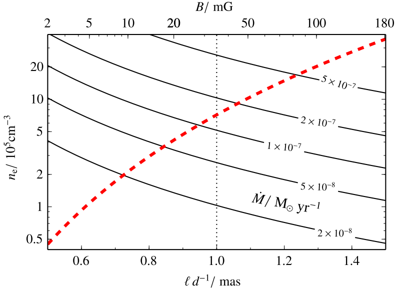

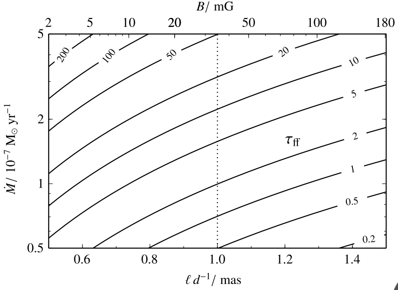

Modeling the LS 5039 spectrum

Building a coherent picture from the fits and the free-free opacity:

- Avg. spectrum: SSA+Razin
- July 19 spectrum: SSA
- July 21 spectrum: SSA+Razin
- Coherent picture with:

$$\ell \sim 0.85 \text{ mas } (\sim 2.5 \text{ AU})$$
$$B \sim 20 \text{ mG}$$
$$n_{\rm e} \sim 4 \times 10^5 \text{ cm}^{-3}$$
$$\dot{M} \sim 5 \times 10^{-8} \text{ M}_\odot \text{ yr}^{-1}$$

where:

ℓ: linear size of the emitting region,

B: module of the magnetic field,

$n_{\rm e}$: electron density of the non-relativistic plasma,

$\dot{M}$: mass-loss rate of the companion star.

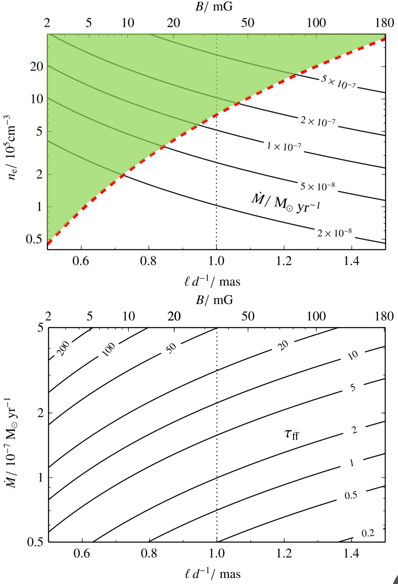

Modeling the LS 5039 spectrum

Building a coherent picture from the fits and the free-free opacity:

- Avg. spectrum: SSA+Razin
- July 19 spectrum: SSA
- July 21 spectrum: SSA+Razin
- Coherent picture with:

$$\ell \sim 0.85\ \mathrm{mas}\ (\sim 2.5\ \mathrm{AU})$$
$$B \sim 20\ \mathrm{mG}$$
$$n_\mathrm{e} \sim 4\times10^{5}\ \mathrm{cm}^{-3}$$
$$\dot{M} \sim 5\times10^{-8}\ \mathrm{M}_\odot\ \mathrm{yr}^{-1}$$

where:

ℓ: linear size of the emitting region,
B: module of the magnetic field,
n_e: electron density of the non-relativistic plasma,
$\dot{M}$: mass-loss rate of the companion star.

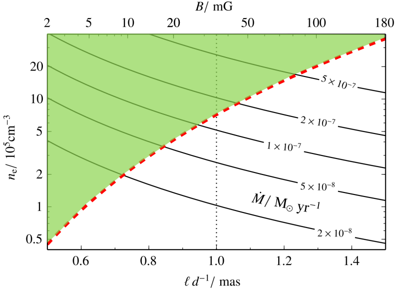

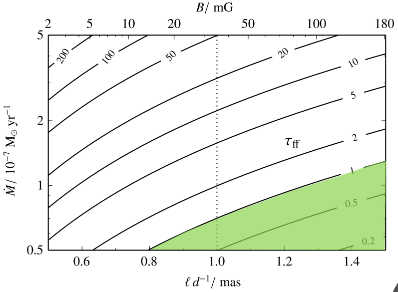

Modeling the LS 5039 spectrum

Building a coherent picture from the fits and the free-free opacity:

- Avg. spectrum: SSA+Razin
- July 19 spectrum: SSA
- July 21 spectrum: SSA+Razin
- Coherent picture with:

$$\ell \sim 0.85 \text{ mas } (\sim 2.5 \text{ AU})$$
$$B \sim 20 \text{ mG}$$
$$n_e \sim 4 \times 10^5 \text{ cm}^{-3}$$
$$\dot{M} \sim 5 \times 10^{-8} \text{ M}_\odot \text{ yr}^{-1}$$

where:

ℓ: linear size of the emitting region,

B: module of the magnetic field,

n_e: electron density of the non-relativistic plasma,

$\dot{M}$: mass-loss rate of the companion star.

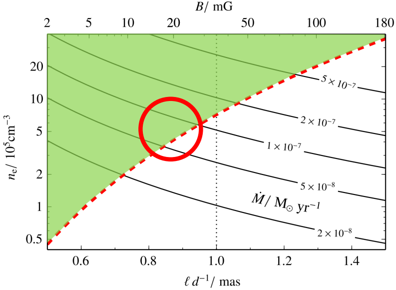

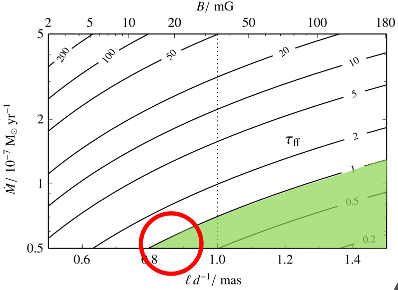

Modeling the LS 5039 spectrum

- A **significant mixing** of the non-relativistic wind inside the synchrotron radio emitting relativistic plasma, even close to ~ 100 %, is observed.

- The derived mass-loss rate (model dependent, in agreement with the last results, Casares, in prep.) implies that the wind is clumpy.

- The presence of Razin effect, widely observed in Colliding Wind Binaries, could give further support to the scenario of the young non-accreting pulsar.

Conclusions

Marcote et al. (2015), MNRAS in press (`arXiv:1504.07253`)

- We report day to day variability, trends on week timescales, and the absence of orbital variability. Variability $< \pm 25$ % is observed at all frequencies (0.23–15 GHz) even on year timescales.
- Persistent turnover at around ~ 0.5 GHz.
- No detection up to now at 150 MHz
- The considered simple model can explains the observed spectra, indicating that the turnover is dominated by SSA
- A contribution of Razin effect is also observed at some epochs.
- Even with this simple model we have obtained a coherent picture that explains the observed spectra.
- Future multifrequency campaigns with more accurate results (specially at low frequencies) are required to compare with more detailed models.

Back-up slides

Razin effect

The synchrotron emission propagates through a plasma, which presents a refractive index n. Always that $n < 1$ the beaming effect is partially suppressed. Although at high frequencies the effect is negligible, at low frequencies (with $\nu \ll \nu_{\rm p}$, where $\nu_{\rm p}$ is the plasma frequency) it suppresses the beaming effect since

$$n^2 = 1 - \left(\frac{\nu_{\rm p}}{\nu}\right)^2$$

and the beaming effect goes as

$$\theta_{\rm b} \approx \gamma^{-1} = \sqrt{1 - n^2\beta^2}$$

- Presence of a thermal plasma surrounding the emitting region.
- Attenuation of the synchrotron radiation at low frequencies.
- Widely reported in Colliding Wind Binaries, solar wind,...
- A good approximation is an exponential attenuation at low frequencies (Dougherty et al. 2003):

$$S_\nu \propto S_\nu e^{-\nu_{\rm R}/\nu}, \qquad \nu_{\rm R} \equiv 20 n_{\rm e} B^{-1}$$